

A simple way to explain phenomena at the event horizon of static black holes

Joachim Pomper, Philipp Schreiner

08.12.2021

Contents

1. Introduction	2
2. Schwarzschild solution	2
2.1. Setup and review of derivation	2
2.2. Critical discussion in terms of charts	4
2.3. Counter-intuitive chart ambiguities	6
3. A non pathological chart	8
3.1. Alternative coordinate systems	8
3.2. Kruskal-Szekeres coordinates	10
3.3. Going back from Kruskal-Szekeres to Schwarzschild	12
4. Free falling particle	13
4.1. Geodesic equation	13
4.2. Initial conditions	15
4.3. Numerical implementation	16
5. The thought experiment	16
5.1. Kruskal-Szekeres Diagramm	17
5.2. Light signals, transeiving times and red shifts	18
5.3. Time orientation	19
5.4. Trajectory in Schwarzschild coordinates	20
A. Conventions	21
B. Lambert W function	21
C. Example of an ambiguous atlas for euclidean space	22

1. Introduction

Black Holes are interesting objects to study. Part of the fascination originates from phenomena close to the black hole's so called event horizon. This is the three dimensional hyper-surface which shields the space-time singularity (believed to be in the center of the black hole) from the rest of space-time. No information about the volume enclosed by this horizon can be obtained from an observer on the outside. This project started out with the (actually rather unscientific) opposite question, namely "Can an observer, falling into the black hole, still obtain information from beyond the horizon, once he passed it". But, by theoretically answering that question, we ended up with a nice little thought experiment, explaining a lot of things in an easy to understand way, that are typically kind of cumbersome. For example the correct, nevertheless confusing, statement, that "an observer outside the horizon will never see matter falling towards the black hole pass the horizon in all eternity". Furthermore, it is sometimes claimed that "time and space change roles when passing the horizon", which we believe to be a confusing misconception. In this little project we will first introduce a typical solution to the Einstein equations, obtained by a symmetry ansatz and explain some phenomena typical to this coordinate system. After pointing out some caveats we discuss some of the other commonly used coordinate systems to describe this problem, focusing on the so called *Kruskal-Szekeres* coordinates. In these coordinates we numerically solve the equations of motion for a free falling massive particle with initial conditions that can be physically interpreted in order to set up a little thought-experiment. With this we present our solution to the initial problem and see how some other phenomena can be demonstrated easily using *Kruskal-Szekeres* coordinates. Lastly, we will lose some words of caution when it comes to working with coordinate systems in general relativity. All our investigations restrict to static (eternal), uncharged black holes. We will mention a non static collapse scenario, but we do not investigate other models like charged or rotation black holes. For the conventions used, see the appendix.

2. Schwarzschild solution

2.1. Setup and review of derivation

The setup for the static, uncharged black hole (BH) scenario is a matter distribution where the majority of mass is concentrated in a tiny spherical portion of space. The matter density outside this region is supposed to be negligible in comparison to the matter density inside. It is therefore reasonable (due to the matter density being effectively isotropic on the outer region) to make an isotropic ansatz for the metric to be determined by the Einstein equations.

$$ds^2 = B(r, t)dt^2 - A(r, t)dr^2 - r^2 \left((d\theta^2 + \sin(\theta)^2 d\phi^2) \right) \quad (2.1)$$

In this ansatz we would like r to have the meaning of a radial coordinate. For that we set $r = 0$ to describes the center of mass of the matter distribution and we need to

impose

$$\lim_{r \rightarrow \infty} A(r, t) = \lim_{r \rightarrow \infty} B(r, t) = 1 \quad \forall t \in (-\infty, \infty) \quad (2.2)$$

in order to correctly model the behavior that gravitational effects of a locally centered mass density are negligible at asymptotic radial distances. This ensures that we can (at least for asymptotically distant observers) interpret t as a time and r as a radial coordinate. The region where the mass is centered can be chosen to be all space-time points with $r < r_0$. Effectively, we model the components of the energy-momentum-tensor (w.r.t. the coordinate system just introduced) on the right hand side of the Einstein equations via

$$T_{\mu\nu}(r, t, \theta, \phi) = 0 \quad \forall r > r_0. \quad (2.3)$$

Birkhoff's theorem then tells us that, for $r > r_0$ the solution of the Einstein equation must also be static, i.e. $B(r, t) = B(r)$ and $A(r, t) = A(r)$. The Einstein equations effectively reduce to

$$R_{\mu\nu} = 0 \quad (2.4)$$

in the region with vanishing matter density. Now, calculating the Ricci curvature tensor from this ansatz leads to the differential equations

$$\frac{R_{00}}{B} + \frac{R_{11}}{A} = -\frac{1}{rA} \left(\frac{1}{B} \frac{dB}{dr} + \frac{1}{A} \frac{dA}{dr} \right) = 0 \quad (2.5)$$

$$R_{22} = r \frac{dB}{dr} + B - 1 = 0. \quad (2.6)$$

The first equation is solved uniquely by

$$A(r)B(r) = 1 \quad (2.7)$$

if one takes the asymptotic behavior (2.2) into account. The second equation is solved by

$$B(r) = 1 - \frac{a}{r} \quad (2.8)$$

with an integration constant a . We obtain the so-called *Schwarzschild metric* for a space-time outside a spherical matter distribution.

$$ds^2 = \frac{r-a}{r} dt^2 - \frac{r}{r-a} dr^2 - r^2 (d\theta^2 + \sin^2(\theta) d\phi^2) \quad (2.9)$$

The value of the integration constant a can again be fixed by looking at the Newtonian limit

$$1 - \frac{a}{r} = B(r) = g_{00} \underset{r \rightarrow \infty}{\approx} 1 - \frac{2GM}{r} \quad (2.10)$$

hence

$$a = 2GM \quad (2.11)$$

where m is the total mass (or equivalently energy) concentrated in the region centered around $r \approx 0$ and G is the gravitational constant. We only reviewed the key steps presented in chapter 24 in the book of T. Fließbach. For a more detailed derivation of the Schwarzschild solution we refer the reader to [1].

This solution is in principle the general relativistic analog to the solution of a spherical gravitational potential, modeling the gravitational field of a star or planet. If we look closely, we see that the metric has a singularity for $r = a$. It is well known that this hyper-surface $r = a$ has physical significance and represents the event horizon of the BH, although it turns out that the singularity is just an artifact of the coordinate choice. We will see all that in a very clear way and therefore postpone the discussion to section ?? . For the Schwarzschild coordinates this singularity for now only means that there are actually two separate solutions to the equations (2.5) and (2.6). Note that this solution only holds true outside the mass distribution e.g. for $r > \max(r_0, a)$. If we are dealing with planets $r_0 > a$ surely holds true. Hence, the coordinate singularity of the metric is not of importance and we only have one relevant solution. But if we are dealing with a BH, we talk about objects whose gravitational field originates from very high energy densities concentrated in a tiny spacial domain hidden behind the horizon. There, we may have to take the solution for $r < a$ into account. As we see later, we cannot interpret r as a radial distance anymore in this regime and the notion of a mass concentrated at $r < r_0$ becomes non valid. We will see that spacetime has a singularity along the $(t, r = 0)$ coordinate line.

2.2. Critical discussion in terms of charts

We first discuss the solution for $r > a$. In this regime we have that $A(r) > 0$ and $B(r) > 0$ and due to (2.2) and (2.10) we can apply our classical physical intuition about gravity for large r . The coordinate t can thus be interpreted as the time an asymptotically far away observer would measure which can be seen from either (2.10) or (2.9). The coordinate r can be interpreted as some radial distance for $r > a$. Now one important thing in general relativity is to think of coordinates in terms of a chart, parametrizing a sub-domain of the (or possibly the whole) space-time. To put it into more mathematical terms: If (t, r, θ, ϕ) are coordinates of a point in the real world, represented by a smooth manifold M , then there exists a homeomorphism

$$\begin{aligned} \Phi_I : U_I &\rightarrow \Phi_I(U_I) \subseteq \mathbb{R}^4 \\ p &\mapsto (t(p), r(p), \theta(p), \phi(p)) \end{aligned} \tag{2.12}$$

where $U_I \subseteq M$ is an open set in M . The domain U_I is the part of the space-time actually covered by these coordinates. A priori, it is not possible to say whether or not our coordinates cover the whole space-time. This is important to keep in mind. We call (U_I, Φ_I) the “Schwarzschild chart of domain I”. The parameter space for this chart is given by the open set

$$\Phi_I(U_I) = (-\infty, \infty) \times (a, \infty) \times (0, \pi) \times (0, 2\pi). \tag{2.13}$$

Lets have a look at the other solution: Here we again must have a chart map

$$\begin{aligned}\Phi_{II} : U_{II} &\rightarrow \Phi_{II}(U_{II}) \subseteq \mathbb{R}^4 \\ p &\mapsto (t(p), r(p), \theta(p), \phi(p))\end{aligned}\tag{2.14}$$

with the parameter space

$$\Phi_{II}(U_{II}) = (-\infty, \infty) \times (0, a) \times (0, \pi) \times (0, 2\pi).\tag{2.15}$$

We call (U_{II}, Φ_{II}) the “Schwarzschild chart of domain II”. But if we try to interpret the coordinate t as time like before, we fail, because we cannot define an asymptotic observer (simply because now the variable r is bounded). A closer further look reveals that t cannot be interpreted as a time because $A(r) < 0$ and $B(r) < 0$ which means that t -coordinate lines actually have no tangent vectors that lies within the light cone. Thus this coordinate cannot be used to define a time. Strangely, the coordinate r can be interpreted as a time-coordinate. But this in contrast makes it impossible to interpret it as a radial distance (this is also the reason why we restricted the mass to a single point). This is sometimes referred to as the *tipping of lightcones*.

Our physical intuition would tell us that the domains I and II described by the coordinates are neighboring parts of the space-time manifold separated only by a hyper-surface and that r and t should therefore have a similar meaning. But actually, we do not know anything about the relation of these two domains. It will later turn out that our intuition was not wrong all along, but in general relativity intuition can lead to very dangerous misunderstandings. One thing that can help out intuition is to visualize the geometry’s geodesics in a chart in order to get a feeling of the dynamics of free falling point-like particles. Null-geodesics give the trajectories of light and can tell us something about causality. In the Schwarzschild chart the null-geodesics are given by

$$t(r) = r + a \ln(|r - a|) + C\tag{2.16}$$

$$t(r) = -r - a \ln(|r - a|) + C.\tag{2.17}$$

In books one then often finds plots like in figure 1, where one visualizes the coordinates of the two charts in one plot, which leads to the illusion that there is some direct connection between the two parameter spaces. But actually there is not! After having a closer look one could try to see the tipping of light cones from the tangent vectors to the null-geodesics. This is illustrated in figure 2. Here, one sees that it’s not really a *tipping*, but rather a discontinuous *flipping*. To be fair, there are coordinate systems, such as *Eddington Finkelstein coordinates* in which this *tipping* can be understood better [2]. It is also important to note that a priori it is not known which of the two possible cones in the domain II gives the correct light cones due to the fact that we cannot carry over the notion of time orientation from I . We will later see why the choice presented in figure 2 is indeed correct. We would like to mention that figure 2 can only be understood qualitatively because strictly speaking it does not make sense to draw tangent vectors as arrows in the parameter space. Before continuing to introduce a new coordinate system which is better suited to describe what’s going on, we would like to lose a few more words of caution when it comes to interpreting coordinate charts in general relativity.

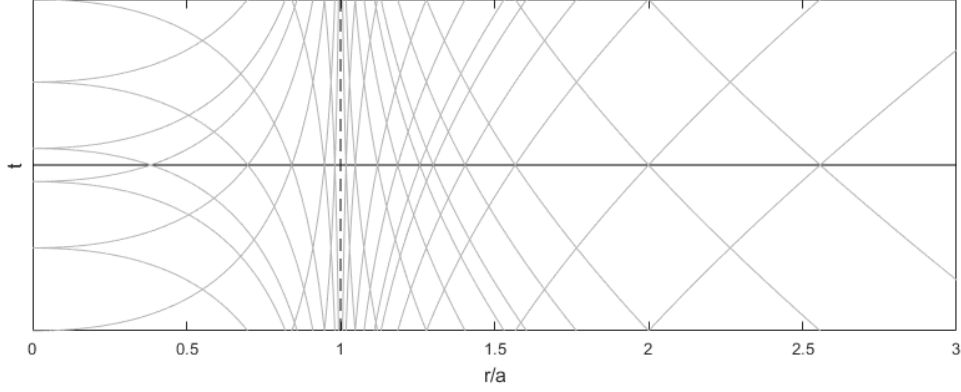


Figure 1: Visualization of the null-geodesics in the Schwarzschild chart.

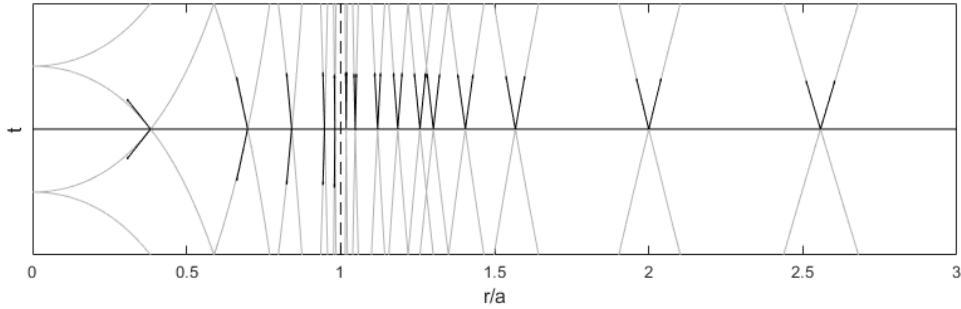


Figure 2: Visualization of flipping of light cones in schwarzschild coordinates.

2.3. Counter-intuitive chart ambiguities

In general relativity we actually formulate most of our theories in charts instead of directly formulating it in terms of abstract objects on the spacetime manifold. Yet being an adequate description of physics accurately implementing how physicists describe the world from different points of view, this can nevertheless also lead to ambiguities which one has to always keep in mind. First and most importantly, that coordinates used for a chart can only be interpreted within one chart by relating them to physics described with these coordinates. Another thing to keep in mind is that just because the parameter domain is the whole \mathbb{R}^4 this does not mean that the coordinate system describes all of spacetime. A chart

$$\begin{aligned}\Phi : U &\rightarrow \Phi(U) = \mathbb{R}^4 \\ p &\mapsto (x^0(p), x^1(p), x^2(p), x^3(p))\end{aligned}\tag{2.18}$$

can in principle cover only a very “small” portion of space-time, nevertheless mapping it to all \mathbb{R}^4 . The last thing to keep in mind is that when it comes to interpreting coordinates, we cannot necessarily interpret coordinates in the same way if they cannot be connected via a continuous path in parameter space. An excellent example is the situation of Schwarzschild coordinates: We discussed above that for a proper description

we actually need to introduce two separate charts. In figure 3 we illustrate an example construction to point out what all can actually go wrong. If we identify the parameter

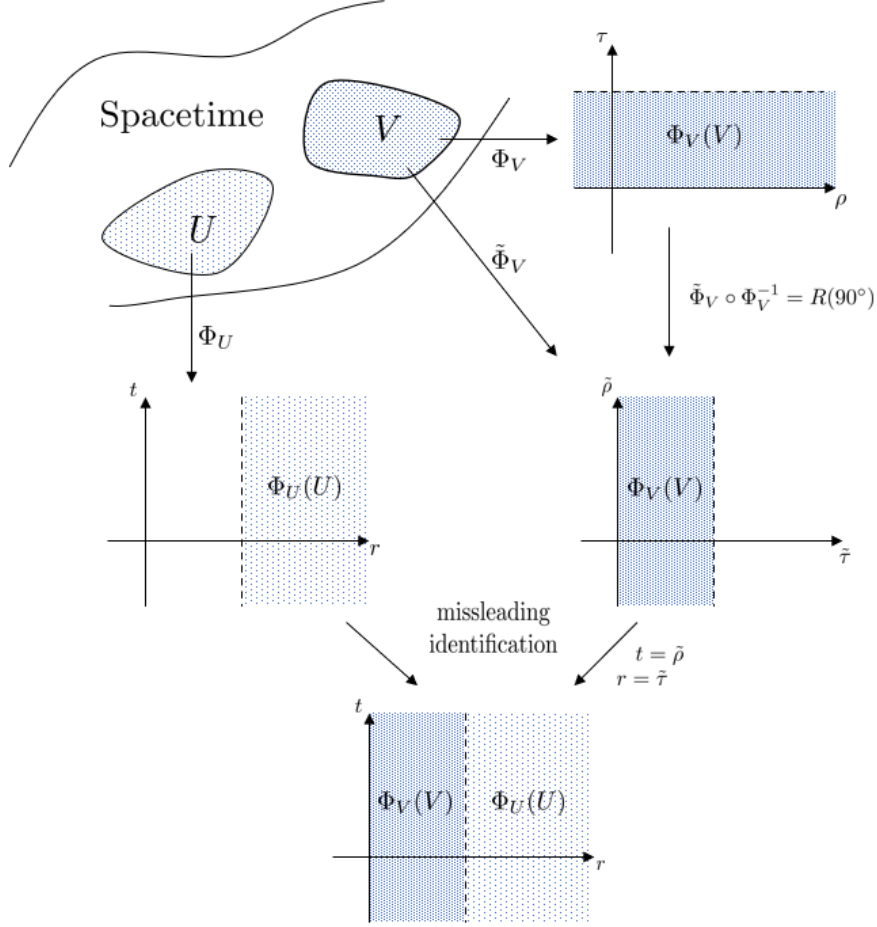


Figure 3: A graphical demonstration of a misleading construction using charts of two separated space-time domains, that might lead to the conclusion that these domains are connected in some sense, when interpreting charts in the wrong way

spaces of two charts as sub-domains of a bigger parameter space, that are only separated by a hyper-surface, one might be led into the idea of these domains being neighboring also on the manifold level. Figure 3 shows that this doesn't have to be the case. Furthermore, we constructed an explicit simple example of a 1d flat manifold in appendix ??, where such a construction of misleading charts is demonstrated explicitly. The only way to safely check the relation of the space-time domains is to find a bigger chart, that at least covers parts of both domains on the manifold level. Such a chart is for example given by the *Kruskal-Szekeres* coordinates and the discussion of this chart will nicely illustrate how all the possible problems and ambiguities discussed here come about in Schwarzschild coordinates. We therefore see that the symmetry ansatz helped us a lot in order to find a solution to the Einstein equations, but the result might not be the best coordinate system to understand the physical implications of the solution.

3. A non pathological chart

The derivation of various coordinate systems follows closely [3], and can also be looked up there.

3.1. Alternative coordinate systems

As already mentioned the *Schwarzschild coordinates* (SSC) are not suitable to describe the physics of a static black hole, because they do not cover the event horizon and potentially do not cover all of spacetime. In the following we will always suppress the angle coordinates ϕ, θ , since all our transformations will only result from a mixing of t and r . We will abbreviate the angular part by $d\Sigma^2$. In order to find a better suited coordinate system we introduce the *tortoise coordinate* $r^*(r)$ defined by

$$\epsilon r^*(r) = r + a \ln \left(\left| \frac{r}{a} - 1 \right| \right) - a = \begin{cases} r + a \ln \left(\frac{r}{a} - 1 \right) - a & \text{for domain I} \\ r + a \ln \left(1 - \frac{r}{a} \right) - a & \text{for domain II} \end{cases} \quad (3.1)$$

where $\epsilon = \pm 1$. From this one could then define the so called *Eddington-Finkelstein coordinates*

$$\tilde{t}(t, r) := t \quad (3.2)$$

$$U(t, r) := t - r^*(r) \quad (3.3)$$

where for $\epsilon = 1$ one speaks of *outgoing Eddington-Finkelstein coordinates* and for $\epsilon = -1$ of *ingoing Eddington-Finkelstein coordinates*. In these coordinates the outgoing/ingoing nullgeodesics are given by the condition $V = \text{const.}$, which can be seen by comparison of (2.16) and (3.1). We will not further concern ourselves with these coordinates, for more information see [2]. We choose now $\epsilon = +1$. With

$$dr^* = \epsilon \left(1 + \frac{a}{\frac{r}{a} - 1} \frac{1}{a} \right) dr = \frac{\epsilon r}{r - a} dr \quad (3.4)$$

it follows for the metric

$$ds^2 = \frac{r - a}{r} dt^2 - \frac{r}{r - a} \left(\frac{\epsilon r}{r - a} \right)^2 dr^{*2} - d\Sigma^2 \quad (3.5)$$

$$= \frac{r(t, r^*) - a}{r(t, r^*)} (dt^2 - dr^{*2}) - d\Sigma^2 \quad (3.6)$$

Next we introduce coordinates that implement a combination of ingoing and outgoing *Eddington-Finkelstein coordinates* called *Tortoise lightcone coordinates*.

$$\tilde{u}(t, r) := t - r^*(r) \quad (3.7)$$

$$\tilde{v}(t, r) := t + r^*(r) \quad (3.8)$$

In these coordinates the outgoing radial null geodesics are parametric by the condition $\tilde{u}(t, r) = \text{const.}$ and the outgoing radial null geodesics are parametric by $\tilde{v}(t, r) = \text{const.}$. The metric becomes

$$ds^2 = \frac{r(\tilde{u}, \tilde{v}) - a}{r(\tilde{u}, \tilde{v})} d\tilde{u} d\tilde{v} - d\Sigma^2 \quad (3.9)$$

Although the identification of radial null geodesics becomes very easy, making it easy to talk about causal relations, the metric is still singular at $r(\tilde{u}, \tilde{v}) = a$. Thus we still have to use two charts and are not able to cover the event horizon. From equation (3.1) it follows

$$\left| \frac{r - a}{a} \right| = \exp \left(\frac{r^*(r) - r}{a} + 1 \right) = \exp \left(\frac{\tilde{v} - \tilde{u}}{2a} \right) \exp \left(\frac{a - r}{a} \right) \quad (3.10)$$

and hence

$$\frac{r - a}{a} = \text{sign} \left(\frac{r - a}{a} \right) \exp \left(\frac{\tilde{v} - \tilde{u}}{2a} \right) \exp \left(\frac{a - r}{a} \right) \quad (3.11)$$

or better

$$\frac{r - a}{r} = \frac{a}{r} \text{sign} \left(\frac{r - a}{a} \right) \exp \left(\frac{\tilde{v} - \tilde{u}}{2a} \right) \exp \left(\frac{a - r}{a} \right) \quad (3.12)$$

With this the metric reads

$$ds^2 = \frac{a}{r} \text{sign} \left(\frac{r - a}{a} \right) \exp \left(\frac{\tilde{v} - \tilde{u}}{2a} \right) \exp \left(\frac{a - r}{a} \right) d\tilde{u} d\tilde{v} - d\Sigma^2 \quad (3.13)$$

Introducing the so-called *Kruskal-Szekeres lightcone coordinates*

$$\begin{aligned} u(t, r^*) &:= -2a \text{sign} \left(\frac{r - a}{a} \right) \exp \left(-\frac{\tilde{u}}{2a} \right) \\ &= -2a \text{sign} \left(\frac{r - a}{a} \right) \exp \left(-\frac{t - r^*}{2a} \right) \end{aligned} \quad (3.14)$$

$$\begin{aligned} v(t, r^*) &:= 2a \exp \left(\frac{\tilde{v}}{2a} \right) \\ &= 2a \exp \left(\frac{t + r^*}{2a} \right) \end{aligned} \quad (3.15)$$

the metric becomes

$$ds^2 = \frac{a}{r(u, v)} \exp \left(\frac{a - r(u, v)}{a} \right) du dv - d\Sigma^2 \quad (3.16)$$

where the function $r(u, v)$ must be determined implicitly. Using (3.10) we obtain.

$$uv = -4a^2 \frac{r - a}{a} \exp \left(\frac{r - a}{a} \right) \quad (3.17)$$

Only if this relation is invertible for $r(u, v)$ the *Kruskal-Szekeres lightcone coordinates* make sense. This in principle restricts the parameter space. The inversion can be

performed using the first branch of the *Lambert W function*, see Appendix B. As shown in the section 3.3, from the domain of this function one infers the restriction

$$uv < \frac{4a^2}{e}. \quad (3.18)$$

From the defining equations (3.14) and (3.15) for the *Kruskal-Szekeres lightcone coordinates* and this restriction (3.18) we can conclude the coordinate values used to describe the domains *I* and *II*. For a summary see table 1. We see, as written in the table, that we do not need the whole parameter space, for which relation (3.17) is invertable. This means that in principle, the coordinates (u, v) can be used to define a chart that covers a larger spacetime domain and analytically continues the description of the already known domains. In this larger chart also the event horizon does not appear as a singularity of the metric. Meaning that the singularity was coordinate induced. We will use this extended coordinates in the following to describe our thought experiment. For the lightcone coordinates we nevertheless cannot interpret u and v as spacelike nor timelike. The coordinate lines are null geodesics.

3.2. Kruskal-Szekeres coordinates

In order to have a “time”- and “space”- coordinate we define the *Kruskal-Szekeres coordinates*

$$T = \frac{u + v}{2} \quad (3.19)$$

$$R = \frac{v - u}{2} \quad (3.20)$$

The metric in this coordinates becomes

$$ds^2 = \Omega(u, v) \left(dT^2 - dR^2 \right) - d\Sigma^2 \quad (3.21)$$

with the “conformal factor”

$$\Omega(u, v) := \frac{a}{r(u, v)} \exp \left(\frac{a - r(u, v)}{a} \right). \quad (3.22)$$

Since $\Omega > 0$, we see that we can indeed interpret T as a timelike coordinate and R as a spacelike coordinate. In the lightcone coordinates the null geodesics were parametrized by the condition $u = \text{const.}$ and $v = \text{const.}$. Therefore the null geodesics in *Kruskal-Szekeres coordinates* are given by

$$T(R) = \pm R + C \quad (3.23)$$

e.g. as straight lines with an 45° angle to the R -axis. The spacetime represented in maximally extended *Kruskal-Szekeres coordinates* are visualized in figure (4). Here we see that the schwarzschild domains *I* and *II* are covered by the chart. The null geodesics

Table 1: Summary of the various coordinate systems.

Name	Coordinates	Parameterspace	Domain <i>I</i>	Domain <i>II</i>
SSC <i>I</i>	(t, r)	$t \in (-\infty, \infty)$ $r \in (a, \infty)$	$t \in (-\infty, \infty)$ $r \in (a, \infty)$	-
SSC <i>II</i>	(r, t)	$r \in (0, a)$ $t \in (-\infty, \infty)$	-	$r \in (0, a)$ $t \in (-\infty, \infty)$
TC <i>I</i>	(t, r^*)	$t \in (-\infty, \infty)$ $r^* \in (-\infty, \infty)$	$t \in (-\infty, \infty)$ $r^* \in (-\infty, \infty)$	-
TC <i>II</i>	(r^*, t)	$r^* \in (-a, \infty)$ $t \in (-\infty, \infty)$	-	$r^* \in (-a, \infty)$ $t \in (-\infty, \infty)$
KSLC	(u, v)	$u \in (-\infty, \infty)$ $v \in (-\infty, \infty)$ $uv < \frac{4a^2}{e}$	$u \in (-\infty, 0)$ $v \in (0, \infty)$	$u \in (0, \infty)$ $v \in (0, \infty)$ $uv < \frac{4a^2}{e}$
KSC	(T, R)	$T \in (-\infty, \infty)$ $R \in (-\infty, \infty)$ $T^2 - R^2 < \frac{4a^2}{2}$	$T \in (-\infty, \infty)$ $R \in (-\infty, \infty)$ $R > T $	$T \in (-\infty, \infty)$ $R \in (-\infty, \infty)$ $T^2 - R^2 < \frac{4a^2}{2}$ $T > R $

e-g- the worldlines of light are given by straight lines parallel to the u - and v - coordinate axes. The initially appearing event horizon of the black hole is given by the $u = 0$ e.g. by the v -coordinate axis. The physical meaning of this event horizon becomes immediately clear in this diagram. No light from a event inside of region I can ever reach an event in II , because the light lines run parallel to the horizon. Thus an observer in region II will never be able to obtain information of an event in II . Also we see that additional

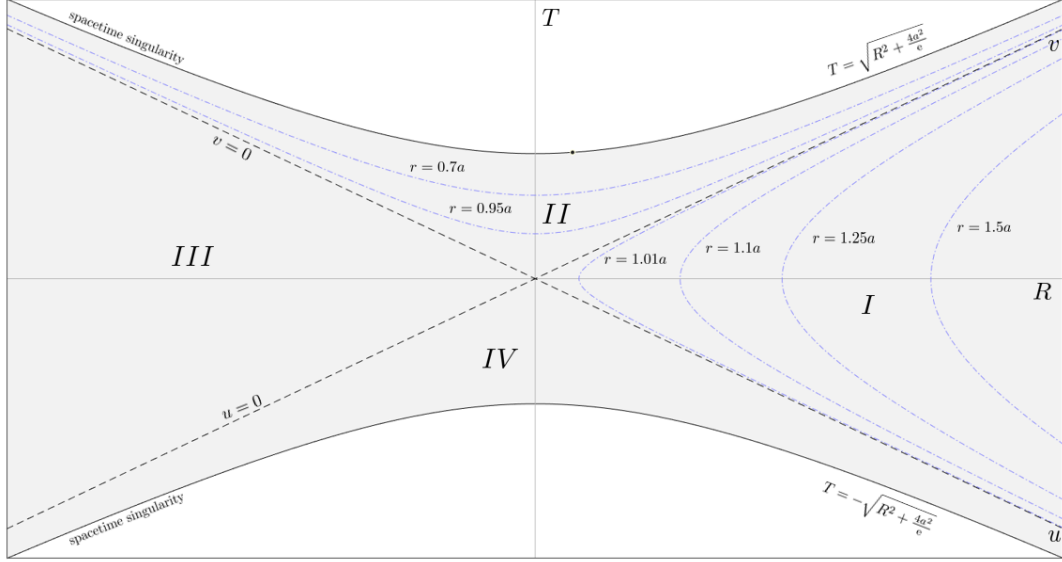


Figure 4: Kruskal-Szekeres coordinate diagram. The schwarzschild domains are label by roman letters. Only the gray area marks the parameters space of the Kruskal-Szekeres coordinates. The blue lines are lines with constant schwarzschild radial component r . The angular components of the coordinate system are suppressed.

spacetime regions III and IV are covered by the chart. These could in principle again be treated by schwarzschild like charts seperatly. Note that only the gray area is really part of the *Kruskal-Szekeres* parameter domain. For parameters corresponding to the white area (3.10) is not invertable for $r(u, v)$.

3.3. Going back from Kruskal-Szekeres to Schwarzschild

In order to go back back we need a relation between u , v and t . Using (3.10) we obtain

$$\frac{v^2}{u^2} = \exp\left(\frac{2t}{a}\right). \quad (3.24)$$

Then the relation $(t(u, v), r(u, v))$ between the coordinates systems SSC and KSLC are described by the implicit equations (3.17) and (3.24). This equations can be solved separately for r and t . The inversion for (3.24) is fairly easy and gives

$$t(u, v) = \frac{a}{2} \ln\left(v^2/u^2\right) \quad (3.25)$$

It is interesting, although not unexpected, to see that the time coordinate diverges at the horizon where $u = 0$ holds. This reminds us that we actually need two different Schwarzschild charts to cover the domains I and II . In order to invert (3.17) for $r(u, v)$ we need to use the first branch of the *Lambert W function* $W_0(z)$.

$$\frac{r - a}{a} = W_0\left(-\frac{uv}{4a^2}\right) \quad (3.26)$$

Since the domain of W_0 is restricted to $z > -e^{-1}$ we can conclude that, in order to be able to invert (3.17), that

$$T^2 - R^2 = uv < \frac{4a^2}{e} \quad (3.27)$$

which was already stated in (3.18). Then the radial schwarzschild coordinate can be written as

$$r(u, v) = a \left(W_0\left(-\frac{uv}{4a^2}\right) + 1 \right) \quad (3.28)$$

We can use this result to explicitly evaluate the metric.

4. Free falling particle

We would like to set up and calculate the following thought experiment: An Astronaut sits in a rocket which is accelerated such that it stays at a constant radial distance (defined in SSC) from the black hole (in order to restrict to a 2 dimensional problem the acceleration is only radial and the rocket has constant zero angular momentum). The astronaut has some device that receives light signals from the rocket and emits signals back to the rocket. We will look now at what happens if the astronaut drops the device into the black hole. In order to do so we have to set up the equations of motion for a free falling massive point like object (in general the geodesic equations for the spacetime) and we have to choose suitable initial condition to find a solution that allows a feasible physical interpretation matching the above thought-experiment. Since the geodesic equation is formulated in coordinates we have to pick a chart. We decide to go with *Kruskal-Szekeers lightcone corrdinates*, since these make the calculation particularly easy and is a maximally extended chart, covering also the horizon. The initial condition are chosen in regular *Kruskal-Szekeers corrdinates*, but the transition is fairly easy. Although the equations look simple, they are quite troublesome and we employ a numerical method to solve them. This comes with some remarks summarized in subsection 4.3.

4.1. Geodesic equation

In order to set up the equation of motion we need the component functions of the metric tensor. We reduce the problem to a two dimensional one, neglecting the angular components. This is a valid reduction since it is well know that in schwarzschild coordinates

purely radial solutions exist.

$$g_{\mu\nu} = \Omega (1 - \delta_{\mu\nu}) \quad (4.1)$$

$$\tilde{g}^{\mu\nu} = \Omega^{-1} (1 - \delta^{\mu\nu}) \quad (4.2)$$

where $\Omega = \Omega(u, v)$ is implicitly defined via (3.22). The Christoffel symbols, given by

$$\Gamma_{\beta\gamma}^{\alpha} = \frac{\tilde{g}^{\alpha\mu}}{2} \left(\frac{\partial g_{\gamma\mu}}{\partial x^{\beta}} + \frac{\partial g_{\beta\mu}}{\partial x^{\gamma}} - \frac{\partial g_{\gamma\beta}}{\partial x^{\mu}} \right) \quad (4.3)$$

$$= \frac{1}{2\Omega} \left(\frac{\partial g_{\gamma|1-\alpha|}}{\partial x^{\beta}} + \frac{\partial g_{\beta|1-\alpha|}}{\partial x^{\gamma}} - \frac{\partial g_{\gamma\beta}}{\partial x^{|1-\alpha|}} \right) \quad (4.4)$$

where $x^0 = u$ and $x^1 = v$. Explicit evaluation results in only two of eight non vanishing Christoffel symbols.

$$\begin{aligned} \Gamma_{00}^0 &= \frac{1}{\Omega} \frac{\partial \Omega}{\partial u} & \Gamma_{11}^1 &= \frac{1}{\Omega} \frac{\partial \Omega}{\partial v} \\ \Gamma_{01}^0 &= 0 & \Gamma_{01}^1 &= 0 \\ \Gamma_{10}^0 &= 0 & \Gamma_{10}^1 &= 0 \\ \Gamma_{11}^0 &= 0 & \Gamma_{00}^1 &= 0 \end{aligned} \quad (4.5)$$

Then derivatives of the conformal factor are calculated to be

$$\begin{aligned} \frac{\partial \Omega}{\partial u} &= -\frac{a}{r} \exp\left(\frac{a-r}{r}\right) \left(\frac{1}{r} + \frac{1}{a}\right) \frac{\partial r}{\partial u} = -\Omega \left(\frac{1}{r} + \frac{1}{a}\right) \frac{\partial r}{\partial u} \\ \frac{\partial \Omega}{\partial v} &= -\frac{a}{r} \exp\left(\frac{a-r}{r}\right) \left(\frac{1}{r} + \frac{1}{a}\right) \frac{\partial r}{\partial v} = -\Omega \left(\frac{1}{r} + \frac{1}{a}\right) \frac{\partial r}{\partial v} \end{aligned}$$

and the derivatives of r are obtained from (3.10) and implicit differentiation.

$$\begin{aligned} v = \frac{\partial uv}{\partial u} &= -4a^2 \exp\left(\frac{r-a}{a}\right) \frac{r}{a^2} \frac{\partial r}{\partial u} = uv \frac{r}{a^2} \left(\frac{r-a}{a}\right)^{-1} \frac{\partial r}{\partial u} \\ u = \frac{\partial uv}{\partial v} &= -4a^2 \exp\left(\frac{r-a}{a}\right) \frac{r}{a^2} \frac{\partial r}{\partial v} = uv \frac{r}{a^2} \left(\frac{r-a}{a}\right)^{-1} \frac{\partial r}{\partial v} \end{aligned}$$

and thus

$$\begin{aligned} \frac{\partial r}{\partial u} &= \frac{a}{u} \frac{r-a}{r} \\ \frac{\partial r}{\partial v} &= \frac{a}{v} \frac{r-a}{r} \end{aligned}$$

Note that the implicit differentiation is possible since we already checked that (t, r) and (u, v) are connected via a diffeomorphism, since they originate from each other by a change of coordinates on the domains I and II respectively. Putting all together gives

$$\Gamma_{00}^0 = -\left(\frac{1}{r} + \frac{1}{a}\right) \frac{a}{u} \frac{r-a}{r} = -\frac{r^2 - a^2}{u r^2} \quad (4.6)$$

$$\Gamma_{11}^1 = -\left(\frac{1}{r} + \frac{1}{a}\right) \frac{a}{v} \frac{r-a}{r} = -\frac{r^2 - a^2}{v r^2} \quad (4.7)$$

Introducing the velocity

$$w^0 := \frac{du}{d\tau} \quad (4.8)$$

$$w^1 := \frac{dv}{d\tau} \quad (4.9)$$

the relativistic free equations of motion

$$\frac{dw^\mu}{d\tau} = -\Gamma_{\alpha\beta}^\mu w^\alpha w^\beta$$

becomes

$$\frac{dw^0}{d\tau} = \frac{r^2 - a^2}{u r^2} (w^0)^2 \quad (4.10)$$

$$\frac{dw^1}{d\tau} = \frac{r^2 - a^2}{v r^2} (w^1)^2 \quad (4.11)$$

The equations (4.8) to (4.11) form a system of four coupled first order ordinary differential equations. The solution to this equation will describe the radial motion of a free falling object with zero angular momentum in schwarzschild spacetime.

4.2. Initial conditions

In order to fix the solution we have to choose initial conditions. But since the coordinates T and R do not allow an intuitive physical interpretation, we have to start from some physical situation we can interpret. To achieve this we assume that the free falling moving object is at first at rest, meaning its schwarzschild radial coordinate $r = r_0 = \text{const.}$ is fixed. If we parametrize the trajectory of this situation and calculate the tangent vector to the curve at time $T = T_0$, we have suitable initial conditions. From (3.17) it follows that the trajectory is given by the condition

$$T^2 - R^2 = -4a^2 \frac{r_0 - a}{a} \exp\left(\frac{r_0 - a}{a}\right) =: -C^2 \quad (4.12)$$

which leads to the parametrization

$$\vec{\gamma}(T) := \left(\frac{T}{\sqrt{T^2 + C^2}} \right) \quad (4.13)$$

where we used the time coordinate T as the curve parameter. In order to calculate the tangent vector with respect to eigentime τ we need

$$d\tau = ds = \sqrt{\Omega} \sqrt{dT^2 + dR^2} = \sqrt{\Omega} \sqrt{1 + \frac{T^2}{T^2 + C^2}} dT = \frac{\sqrt{\Omega} C^2 dT}{\sqrt{T^2 + C^2}} \quad (4.14)$$

and then we obtain

$$\frac{d\vec{\gamma}}{d\tau} = \frac{dT}{d\tau} \frac{d\vec{\gamma}}{dT} = \frac{\sqrt{T^2 + C^2}}{\sqrt{\Omega} C^2} \left(\frac{1}{\frac{T}{\sqrt{T^2 + C^2}}} \right) \quad (4.15)$$

Hence we can choose the following initial conditions

$$u(0) = T_0 - \sqrt{T_0^2 + C^2} \quad (4.16)$$

$$v(0) = T_0 + \sqrt{T_0^2 + C^2} \quad (4.17)$$

$$w^0(0) = \frac{\sqrt{T_0^2 + C^2}}{\sqrt{\Omega} C^2} \left(1 - \frac{T_0}{\sqrt{T_0^2 + C^2}} \right) \quad (4.18)$$

$$w^1(0) = \frac{\sqrt{T_0^2 + C^2}}{\sqrt{\Omega} C^2} \left(1 + \frac{T_0}{\sqrt{T_0^2 + C^2}} \right) \quad (4.19)$$

Which are completely determined by the choice of $C > 0$ and T_0 .

4.3. Numerical implementation

The equations (4.10) and (4.11) can easily be solved numerically, using an explicit Runge-Kutta method. But close to the event horizon, where $u = 0$ holds, numerical problems occur. Fortunately, close to $u = 0$ the function $r(u, v)$ can be rewritten using the convergent series expansion of the Lambert W function (see Appendix B).

$$\tilde{W}_0(u, v) := \frac{W_0\left(-\frac{uv}{4a^2}\right)}{uv} = - \sum_{k=1}^{\infty} \frac{u^{k-1} v^{k-1}}{(4a)^k} \frac{k^{k-1}}{k!} \quad (4.20)$$

This modified Lambert function can be implemented numerically again. We further see that

$$\begin{aligned} \frac{r^2 - a^2}{r^2 u} &= \frac{a^2}{r^2 u} \left(\left(W_0\left(-\frac{uv}{4a^2}\right) + 1 \right)^2 - 1 \right) \\ &= \frac{a^2}{r^2 u} \left(W_0^2\left(-\frac{uv}{4a^2}\right) + 2W_0\left(-\frac{uv}{4a^2}\right) \right) \\ &= \frac{a^2 v}{r^2} \left(W_0\left(-\frac{uv}{4a^2}\right) + 2 \right) \tilde{W}_0(u, v). \end{aligned} \quad (4.21)$$

With this reformulation no numerical problems occur. Note that the series expansion can only be used for

$$|uv| < \frac{4a^2}{e} \quad (4.22)$$

5. The thought experiment

Now, after having discuss all this head on to the initially presented thought experiment of the astronaut dropping a transceiver probe into the black hole. For a proper descriptions we use the previously introduced *Kruskal-Szekeres coordinates*.

5.1. Kruskal-Szekeres Diagramm

Lets consider an astronaut in a rocket ship, whose thruster engine accelerates him in such a way that his spatial schwarzschild coordinates $(r_{\text{rocket}}, \phi_{\text{rocket}}, \theta_{\text{rocket}})$ are kept constant. This allows to reduce the problem to a two dimensional one. The worldline of the rocket ship in *Kruskal-Szekeres coordinates*, characterized by $r_{\text{rocket}} = 1.2a$, is given by (4.13). In figure 5 the rockets trajectory is represented by the blue dashed-dotted line. At “time” $T = 0$ the astronaut drops his transceiver device from the space ship and tracks it falling into the black hole. The trajectory of the probe is plotted in figure 5 as a blue solid line. We see that the probe actually crosses the event horizon after some finite

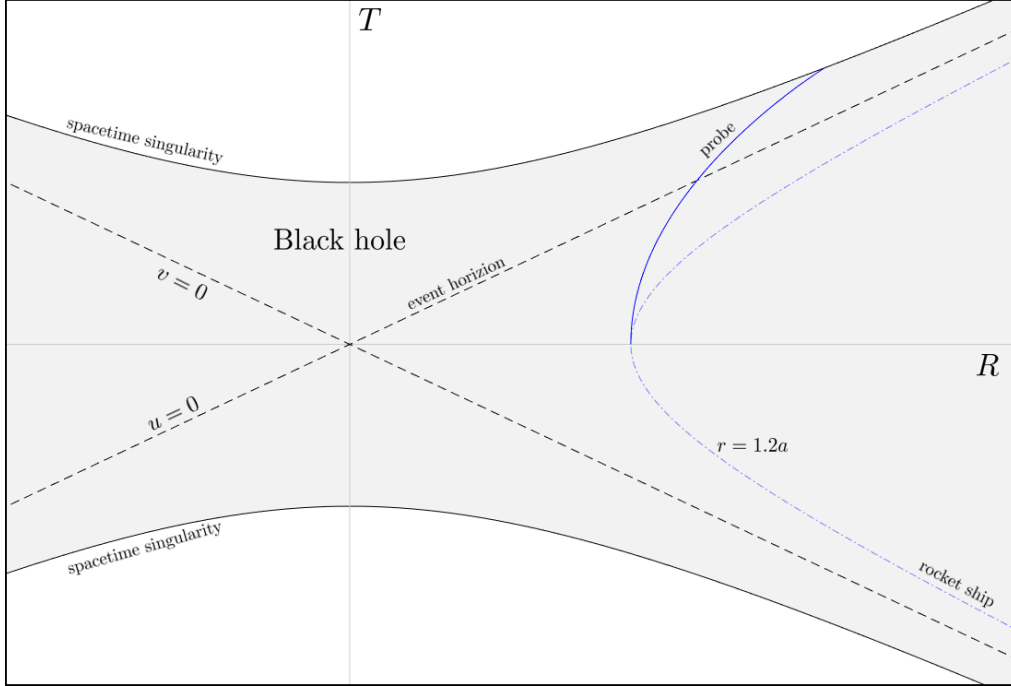


Figure 5: Thought experiment in the Kruskal-Szekeres coordinate diagram. The blue dashed-dotted line represents the rocket ships worldline. The blue line represents the probes worldline, falling into the black hole.

time. Afterwards the trajectory goes on inside the black hole region, never leaving it, destined to end up at the space time singularity. Light, sent from the rocket ship toward the black hole, runs along -45° straights, thus reaching the probe, even if it already passed to event horizon. Nevertheless, because light sent in the opposite direction runs along 45° straights, the light signal from the probe will never reach anything outside the black hole because it runs parallel to the horizon. This is also nicely illustrated in figure 6. Hence we can conclude that objects beyond the event horizon can still receive information from outside the black hole, but no information from the inside will ever reach an outside observer. To understand what out the astronaut in the rocket observes, we have to consider that actually the only way to obtain information about the probe is that he receives a light signal coming from the probe.

5.2. Light signals, transceiving times and red shifts

If the probe passed the horizon, the observer will not be able to receive any signal. But, as illustrated in figure 6, the reflected light signal intersects the worldline of the rocket asymptotically late if the probe is infinitesimally close to the horizon. In order to see that the observer never receives the signal that the probe crossed the horizon in a finite span of eigentime a simple estimate of the eigentime in combination with a geometric interpretation suffices. Nevertheless we would like to calculate the passed spans

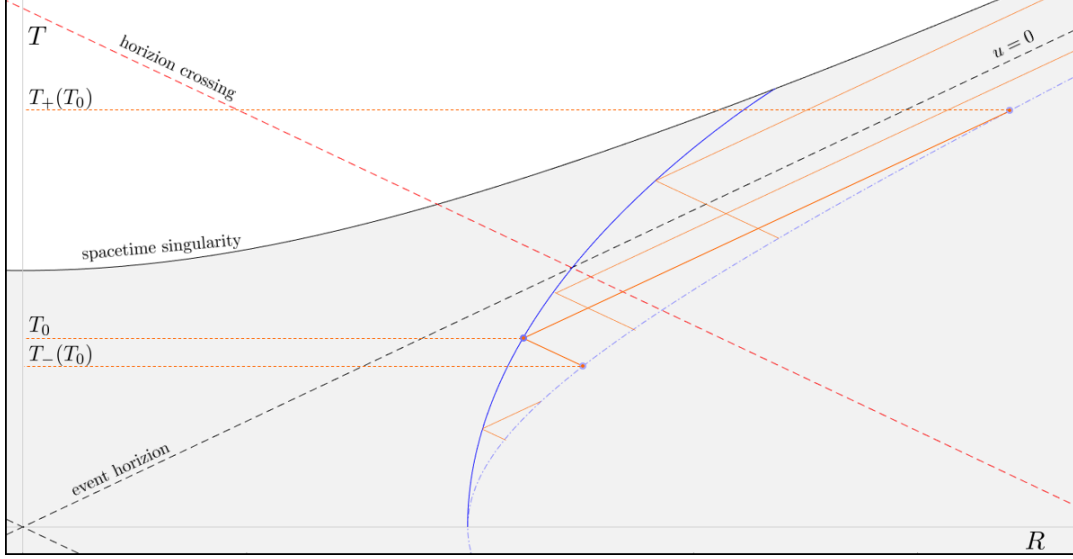


Figure 6: Illustration of how to determine the running of transceived light signals between rocket and probe.

of eigentime between transceived signals exactly. To do so we look $\pm 45^\circ$ straight lines, starting from the probe's trajectory at (T_0, R_0) and where they intersect with the trajectory of the rocket, given by (4.13).

$$\begin{pmatrix} \pm(T - T_0) + R_0 \\ T \end{pmatrix} = \begin{pmatrix} T \\ \sqrt{T^2 + C^2} \end{pmatrix} \quad (5.1)$$

Solving this condition leads to

$$T_+ = \frac{C^2 - (R_0 - T_0)^2}{2(R_0 - T_0)^2} \quad (5.2)$$

$$T_- = \frac{(R_0 + T_0)^2 - C^2}{2(R_0 + T_0)^2} \quad (5.3)$$

In order to obtain the passed proper time between transmitting and receiving a signal, we have to integrate up (4.14).

$$\Delta\tau = \sqrt{\Omega C^2} \int_{T_-}^{T_+} \frac{dT}{\sqrt{T^2 + C^2}} = \sqrt{\Omega C^2} \left(\sinh^{-1} \left(\frac{T_+}{C} \right) - \sinh^{-1} \left(\frac{T_-}{C} \right) \right) \quad (5.4)$$

We used that $\Omega(r) = \Omega(r_{rocket})$ is a constant along the rockets trajectory. This shows that, since T_- finite at the event horizon, in contrast to T_+ , that a signal reflected at the event horizon will never reach the Astronaut in finite time. Finally we can try to think about gravitational red shifts of light signals, omitting Doppler effects. Since we deal with a static spherical symmetric space time, the red shift only depends on the radial distance between the transmitted and received signal. Therefore, perfectly reflected light signals should come back to the astronaut with the same wavelength as they were sent to the probe. But there will be a shift in wavelength for a signal sent from the probe to the rocket. The red shift is given by

$$z = \sqrt{\frac{g_{00}(r_{rocket})}{g_{00}(r_{probe})}} - 1 \quad (5.5)$$

The derivation of this formula can be looked up for example in [1]. The above symmetry argument manifest in *Schwarzschild coordinates*, thus we need to use the metric components with respect to these. Using (2.9) we obtain

$$z = \sqrt{\frac{(r_{rocket} - a)r_{probe}}{(r_{probe} - a)r_{rocket}}} - 1 \xrightarrow{r_{probe} \rightarrow a} \infty \quad (5.6)$$

This expression then obviously diverges if the probe is too close to the event horizon, leading to an infinite red shift of the light signal.

5.3. Time orientation

A time orientation on a space time manifold M is defined as a globally, everywhere non vanishing vector field \mathcal{T} saturating

$$g(\mathcal{T}, \mathcal{T})(P) > 0 \quad \forall P \in M. \quad (5.7)$$

Such a global vector field allows to consistently choose a light cone, out of the double null cone of the metric, defining a proper notion of causality on the space time. While this was problematic to define for the two separated Schwarzschild domain, because the chart did not overlap, no problem occurs in *Kruskal-Szekeres coordinates*. A possible choice would be the vector field of tangent vectors to the T -coordinate lines

$$\mathcal{T} = \frac{\partial}{\partial T} \quad (5.8)$$

After having defined a vector field globally, the notion of time orientation can be taken over in other charts, giving us the proper time orientation and light cones in Schwarzschild coordinates. Using the vector field (5.8) we know to choose the light cones in Schwarzschild coordinates, as we did in figure 2. Simply because with progressing eigentime the particle has to run towards the singularity at $r = 0$. This also connects to the result represented in figure 7.

5.4. Trajectory in Schwarzschild coordinates

Using (3.25) and (3.28) one can easily map the trajectory of the free falling probe back to schwarzschild coordinates. This is shown in figure 7. There one can see that the probe worldline approaches infinite time while getting infinitesimally close to the event horizon. Keeping in mind that schwarzschild coordinate time is the eigen time of an

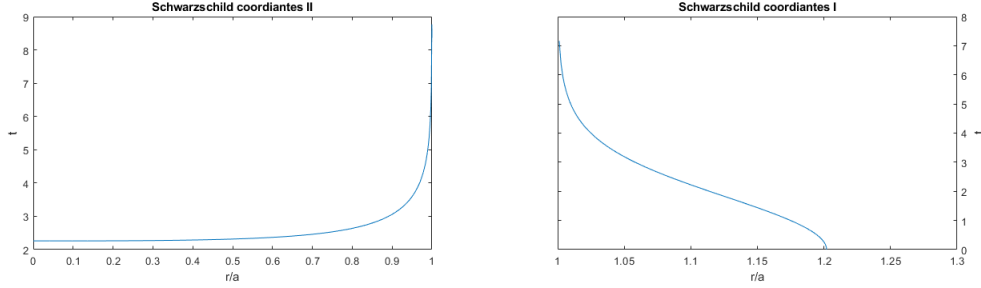


Figure 7: Trajectory of free falling probe in schwarzschild coordinates

asymptotic observer, this is in good agreement with the calculation we did before and can be understood in the same way. Nevertheless, the probe actually crosses the horizon and reaches the singularity after finite eigentime.

A. Conventions

We use the spacetime signature convention

$$\eta_{00} = -\eta_{11} = -\eta_{22} = -\eta_{33} = 1 \quad (\text{A.1})$$

we use a system of units where

$$c = 1 \quad (\text{A.2})$$

holds.

B. Lambert W function

The *Lambert W function* W is defined as the inverse of the function

$$\begin{aligned} M : \mathbb{R} &\rightarrow (-e^{-1}, \infty) \\ x &\mapsto xe^x \end{aligned} \quad (\text{B.1})$$

Since the function $M : \mathbb{R} \rightarrow (-e^{-1}, \infty)$ is not injective on \mathbb{R} one has to defined the

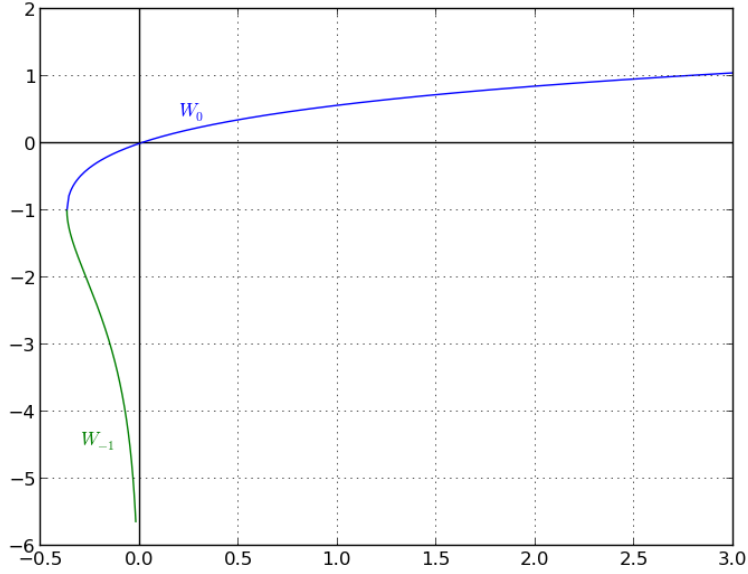


Figure 8: The two branches of the *Lambert W function*. W_0 is called the *first branch*.

inverse on two domains, giving two branches. The branches of the *Lambert W function* are plotted on figure 8. For $|x| < e^{-1}$ the first branch of the *Lambert W function* can be defined by the series expansion

$$W_0(x) := \sum_{k=1}^{\infty} \frac{(-k)^{k-1}}{k!} x^k \quad (\text{B.2})$$

C. Example of an ambiguous atlas for euclidean space

We would like to show that it is possible, by explicit construction, that even for flat 1-dimensional euclidean space a bad choice of coordinates can lead to ambiguous interpretation if not kept in mind that a coordinate system actually corresponds to a chart of the atlas of the spacetime manifold.

As such an example consider the manifold

$$M = (\mathbb{R}, \mathcal{O}_{std}, \mathcal{A}^+, g) \quad (C.1)$$

with \mathcal{O}_{std} the standard topology on \mathbb{R} and g the euclidean metric. The Atlas is given by

$$\mathcal{A}^+ = \{(U_x = \mathbb{R}, x), (U_y = (1, 2), y), (U_z = (-1, 0), z)\} \quad (C.2)$$

with the chart maps

$$\begin{aligned} x : U_x &\rightarrow \mathbb{R} \\ p &\mapsto p \end{aligned} \quad (C.3)$$

$$\begin{aligned} y : U_y &\rightarrow (a, \infty) \subset \mathbb{R} \\ p &\mapsto \frac{a}{1 - (p - 1)^2} \end{aligned} \quad (C.4)$$

$$\begin{aligned} z : U_z &\rightarrow (0, a) \subset \mathbb{R} \\ p &\mapsto a(1 - p^2) \end{aligned} \quad (C.5)$$

where a is some fixed real positive number. The chart $(U_x = \mathbb{R}, x)$ is actually the so-called *canonical chart* of \mathcal{R} . It is a global chart and the metric is completely specified by its chart representation with respect to this chart.

$$g = g_{11,(x)} dx = 1 dx = dx \quad (C.6)$$

It can easily be checked that the charts given are indeed homeomorphisms with respect to the standard topology on \mathbb{R} . The inverse maps are

$$\begin{aligned} x^{-1} : \mathbb{R} &\rightarrow U_x \\ \alpha &\mapsto \alpha \end{aligned} \quad (C.7)$$

$$\begin{aligned} y^{-1} : (a, \infty) &\rightarrow U_y \subset \mathbb{R} \\ \alpha &\mapsto 1 + \sqrt{1 - \frac{a}{\alpha}} \end{aligned} \quad (C.8)$$

$$\begin{aligned} z^{-1} : (0, a) &\rightarrow U_z \subset \mathbb{R} \\ \alpha &\mapsto -\sqrt{1 - \frac{\alpha}{a}} \end{aligned} \quad (C.9)$$

In order to check that this is indeed at least a \mathcal{C}^1 -compatible atlas one has to look at all the possible derivatives of the chart transition functions

$$\begin{aligned} y \circ x^{-1} : (1, 2) &\rightarrow (a, \infty) & z \circ x^{-1} : (-1, 0) &\rightarrow (0, a) \\ x \circ y^{-1} : (a, \infty) &\rightarrow (1, 2) & x \circ z^{-1} : (0, a) &\rightarrow (-1, 0) \end{aligned}$$

given by

$$\begin{aligned} \left. \frac{d y \circ x^{-1}}{d\alpha} \right|_{\alpha=\beta} &= \frac{2a(\beta-1)}{\beta(\beta-2)^2} & \beta &\in (1, 2) \\ \left. \frac{d x \circ y^{-1}}{d\alpha} \right|_{\alpha=\beta} &= \frac{a}{2\beta^2 \sqrt{1 - \frac{a}{\beta-2}}} & \beta &\in (a, \infty) \\ \left. \frac{d z \circ x^{-1}}{d\alpha} \right|_{\alpha=\beta} &= -2a\beta & \beta &\in (-1, 0) \\ \left. \frac{d x \circ z^{-1}}{d\alpha} \right|_{\alpha=\beta} &= \frac{1}{2a \sqrt{1 - \frac{\beta}{a}}} & \beta &\in (0, a) \end{aligned}$$

which are all smooth functions on the respective domains. The superscript + indicates that this atlas is also an oriented atlas. The metric can be expressed particularly in each of the other, non canonical charts

$$\begin{aligned} g = dx &= \frac{dx}{dy} dy = \left. \frac{d x \circ y^{-1}}{d\alpha} \right|_{\alpha=y} dy = \frac{a}{2y^2 \sqrt{1 - \frac{a}{y-2}}} dy = g_{11,(y)} dy \\ g = dx &= \frac{dx}{dz} dz = \left. \frac{d x \circ z^{-1}}{d\alpha} \right|_{\alpha=z} dz = \frac{1}{2a \sqrt{1 - \frac{z}{a}}} dz = g_{11,(z)} dz \end{aligned}$$

In figure 9 the metric component function is plotted over each parameter space for the charts respectively. If one now wrongfully combines these two plots into one, as illustrated in figure 10, the illusion occurs that, if the singularity could be tress passed, the domains, described by the coordinates on the left and the right of the metric singularity, are “near by”. But actually these domains have nothing to do with each other on the manifold itself and are separated by an interval of finite length. Also the singularity is only coordinate induced. Actually our manifold is flat and very simple. Also note that the chart $(U_y = \mathbb{R}, y)$ uses a “infinitely” large parameter space to actually describe an interval of finite length. This illustrates that that, only because our parameter domain is all of \mathbb{R} , we can not conclude that we describe all of spacetime. When using Schwarzschild coordinates to describe the spacetime of a static uncharged black hole, we deal with a similar situation.

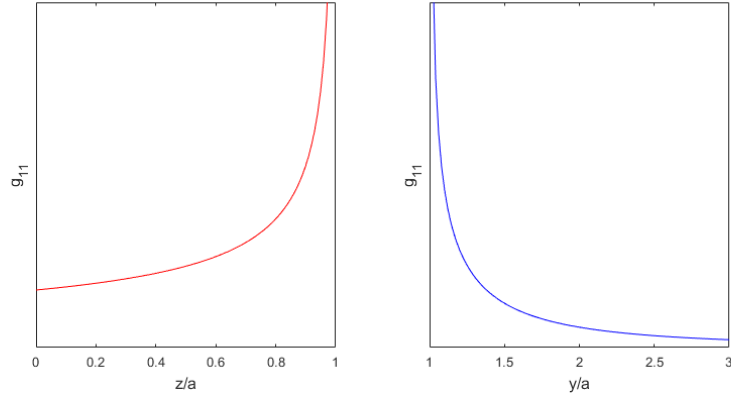


Figure 9: Metric component function g_{11} plotted respective parameter space.

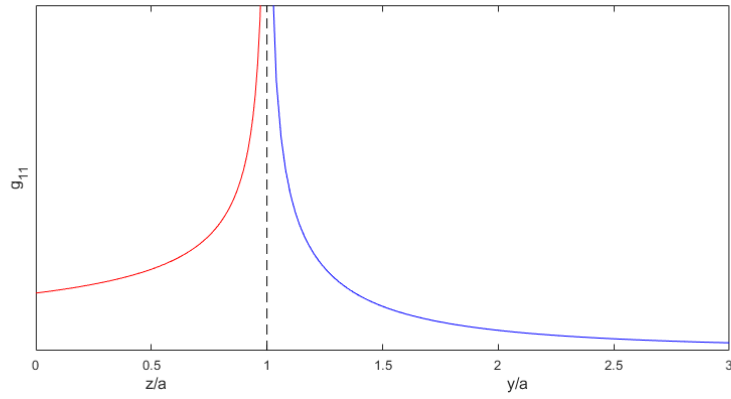


Figure 10: Metric component function g_{11} plotted over a wrongfully combined parameter space.

References

- [1] T. FLIESSBACH. *Allgemeine Relativitätstheorie*. Springer eBook Collection. Springer Spektrum, Berlin, Heidelberg, 7. Aufl. 2016 Auflage, 2016.
doi:10.1007/978-3-662-53106-8
- [2] C. W. MISNER, K. S. THORNE, J. A. WHEELER. *Gravitation / Charles W. Misner, Kip S. Thorne, John Archibald Wheeler*. W. H. Freeman San Francisco, 1973.
- [3] V. MUKHANOV, S. WINITZKI. *Introduction to quantum effects in gravity*. Cambridge university press, 2007.